Prototropic studies in vitreous and in solid phases: Pyranine and 2-naphthol excited state proton transfer

ARTICLE *in* JOURNAL OF LUMINESCENCE · FEBRUARY 2014

Impact Factor: 2.72 · DOI: 10.1016/j.jlumin.2013.09.038

Journal of Luminescence 146 (2014) 57–63

Contents lists available at ScienceDirect

Journal of Luminescence

journal homepage: www.elsevier.com/locate/jlumin

Prototropic studies in vitreous and in solid phases: Pyranine and 2-naphthol excited state proton transfer

Fátima Aparecida das Chagas Silva [a], Eduardo Triboni Rezende [d], Décio Briotto Filho [b], Daisy de Brito Rezende [a], Iolanda Midea Cuccovia [b], Ligia Ferreira Gome [c], Mauro Francisco Pinheiro da Silva [a], Mário José Politi [b,*]

[a] Departamento de Química Fundamental, Faculdade de Ciências Farmacêuticas, Universidade de São Paulo, SP, Brasil
[b] Departamento de Bioquímica Instituto de Química, Faculdade de Ciências Farmacêuticas, Universidade de São Paulo, SP, Brasil
[c] Departamento de Análises Clínicas, Faculdade de Ciências Farmacêuticas, Universidade de São Paulo, SP, Brasil
[d] Universidade Nove de Julho, São Paulo, SP, Brasil

ARTICLE INFO

Article history:
Received 28 June 2013
Received in revised form
11 September 2013
Accepted 17 September 2013
Available online 26 September 2013

Keywords:
Excited State proton Transfer in Glasses
Pyranine
2-Naphthol
Water mole fraction

ABSTRACT

Excited state proton transfer processes in vitreous glasses and in solid mixtures are investigated by steady state fluorimetry and laser flash photolysis kinetic studies with the photoacids pyranine and 2-naphthol. Glasses were derived from TEOS by the sol–gel condensation process and hydrated solid mixtures from NaCl or KH_2PO_4/K_2HPO_4 crystals. The extent of the water content necessary for the reaction is determined. Shrinkage of TEOS derived monoliths from water loss leads to an increase in proton transfer extent due to the increase in local concentrations of accepting and donor buffer species, but the concomitant increase in the ionic strength actuates in an opposite direction. Furthermore, water losses by aging of air-exposed gel goes to a critical 20% weight fraction, beyond it proton transfer reactions are hindered. Similar studies with solid NaCl or solid phosphate buffer mixtures demonstrated the same critical water level indicating that free water molecules are crucial for the proton to escape from the original cage where the geminate ion pair **[–ǁRO$^-$*H$^+$ǁ–]** is formed and can undergo coupled proton transfer reactions.

1. Introduction

Proton transfer reactions are a cornerstone of modern chemistry and biochemistry. Among the systems suited for accompanying the H^+ transfer reactions, photoacids in general and 8-hydroxi-1,3,6-trisulphonatepyrene (pyranine) and 2-naphthol (NOH) more specifically, are very attractive mostly because of the convenient colors of the acid base pairs and the possibilities to follow either stationary state or time resolved measurements. Studies using pyranine and related compounds on excited state proton transfer (ESPT) started with the work by Förster and by Weller in the late fifties and sixties [1,2].

Previous studies on ESPT is sol–gel derived from tetraethyl (TEOS) and tetramethyl (TMOS) orthosilicates having pyranine as the H^+ sensor arrived to the conclusion that after some days of aging exposed to air, water is adsorbed back into the gel as seen by the extent ESPT [3–6]. However, the effects of: (i) increase in the concentration of H^+ donor and accepting species, (ii) increase in the local ionic strength (μ), and (iii) the water content were not considered in detail. In the present study these effects are addressed. The effect of increased ionic strength due to shrinkage (decrease in the water mole fraction) of the gel by aging in the prototropic process and the decrease in the water mole fraction are highlighted. Studies of H^+ transfer in crushed solid salts as a function of the water content are also presented. The study shows that the understanding of the participation of water concentration added to the increase in the ionic strength and in the approximation of donor and accepting proton species must be taken in account for exploitation of H^+ reactions.

2. Background

2.1. Photoacids

Pyranine and 2-naphthol properties can be reviewed elsewhere [1–5], for the sake of clarity pyranine's more important features are included here (relevant properties of 2-naphthol will be included in the results section). Pyranine is a weak acid in the ground state ($pKa=8.2$ at limiting ionic strength (μ)=0) [5] whereas it is a strong one in the excited state ($pKa_{(\mu=0)}=1.3$ [5]). In aqueous medium the lifetime of both excited species (acid

* Corresponding author. Tel.: +55 11 30913814; fax: +55 11 3815 55 79.
E-mail address: mjpoliti@usp.br (M.J. Politi).

0022-2313/$ - see front matter © 2013 Elsevier B.V. All rights reserved.
http://dx.doi.org/10.1016/j.jlumin.2013.09.038

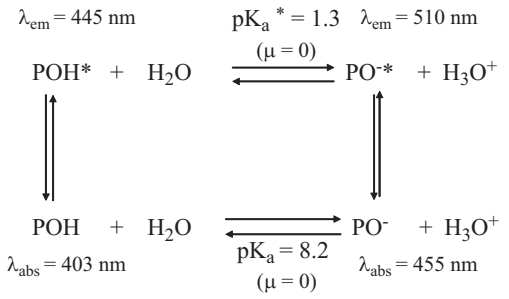

Scheme 1. Prototropic properties of Pyranine acid (POH) and basic (PO^-) species. (symbols have their usual meanings).

and conjugate base) are long enough (~6 ns [1–3]) to ensure a quasi equilibrium condition, that is, ESPT occurs before excited state deactivation. These properties are thus very suitable to monitor the surroundings proticity conditions. Scheme 1 depicts the most relevant properties of pyranine as absorption and emission wavelengths of ground and excited states species and pKa's.

3. Materials and methods

Pyranine (Eastman, Kodak) was dissolved in bidistilled Milli-Q water, stock solutions were prepared routinely and kept cold (~8 °C) and in dark. 2-Naphthol solutions were prepared daily in ethanol and kept in dark. The dye pH indicators Bromophenol Blue (BPB), Bromocresol Green (BCG), Bromocresol Purple (BCP), Cresol Red (CR) and Bromothymol Blue (BTB) (Sigma-Aldrich) were solubilized in ethanol and few microliters were added to the sols for spectrophotometric monitoring the eventual changes in pH's. Buffer solutions were prepared from KH_2PO_4 and NaOH. Tetraethylorthosilanes 98% (TEOS) were from Acros Organics. The liquid stock jar was kept under N_2 atmosphere in a freezer. Polystyrene plastic 1 cm path length cuvettes having all faces polished were used thoroughly. In experiments with solid KH_2PO_4/K_2HPO_4, samples were weighed from vacuum desiccated solids and mixed in the proper amounts into a homemade quartz chamber. Following, the photoacids probes and water (microliters fractions) were added. Water molar fractions (X_w) are mass (weight) based calculated. All reagents were from the best analytical grade available and used without further purifications.

3.1. TEOS sol–gel monoliths preparation.

Hydrolysis of a TEOS:H_2O (mole ratio 1:4) in 2 mM HCl was accomplished with a tip sonifier (Braun Sonic 1510 and 150 mW). This pre-hydrolysis step was continued until a homogeneous and translucent one-phase mixture was obtained. The mixtures were kept in ice to avoid a too fast gelation processes [6–8]. Following, buffer, pH dyes (typically 40 μL) or pyranine (20 μL) totalizing 1.5 mL were added to 1.5 mL of the TEOS hydrolyzate onto the plastic cells in a Branson water bath sonifier to ensure good mixing. Given the pre-hydrolysis condition and the fact that high buffer (electrolytes in general) concentrations (> 0.5 M) lead to a powdery gel, buffer concentrations were kept below 250 mM. In these conditions there is an inherent change in the pH as will be presented below. For this reason pH dyes were used with the gels to spectrophotometrically monitor the H^+ concentration as a function of aging (see below). All samples were kept exposed to air in dark and with a temperature of ~25 °C. Mole ratio of TEOS: H_2O was 1:18. The pH dye and pyranine concentrations in the assays were 10 μM and 50 μM respectively.

Solid mixtures were prepared by weighing the appropriate amounts of KH_2PO_4 and $K_2H\ PO_4$ for a nominal pH as presented in the figure captions. The mixtures were grinded in a mortar, doped with either pyranine or 2-naphthol and dried in vacuum for about 1 h at ~150 °C. NaCl samples were doped with pyranine and dried for the phosphate samples.

UV–vis and fluorescence spectra were obtained in a Cary 300 spectrophotometer and a Hitachi F-200, respectively. For the fluorescence measurements a work tension of 400 V was applied to the PM tube and fixed slits of 10 mm were used (bandwidth=26 nm, according to the fabricant). Pyranine emission spectra were collected from 420 nm to 600 nm keeping the excitation at 350 nm. With these conditions, scattering and Raman contributions were minimized. For the solid mixtures after drying, the samples were deposited on a quartz slide and another slide mounted on top of it. Solid samples were prepared by grinding the solids in a mortar. Powders were kept dry in vacuum desiccators. Appropriate aliquots of the solutions were mixed with the powders before pressing them with another quartz slide for frontal angle measurements in the fluorometer.

Laser flash photolysis measurements were conducted with an Applied Photophysics system composed of a Nd:YAG laser delivering light pulses width of ~50 ns (FWHM), using the 3rd harmonic (355 nm) and a working power of 20 mJ/pulse. In this condition photo-oxidation of pyranine was almost none (complete recovery of the o'scope traces to the pre pulse level were observed). Transients were monitored by a Xenon pulsed lamp either in a parallel or perpendicular configurations and presented the same results. Data were stored in a digital o'scope (HP 54510C) and transferred to a PC like computer for data handling and treatment.

Overall typical instrumental and experimental errors are within 4–7%.

4. Results and discussions

4.1. pH's in TEOS monoliths

In the TEOS derived glasses prepared in this study, besides the photoacid species, other acid and bases included in the gel are the phosphate buffer and the pH sensitive dyes. Previous studies showed that pH indicators (HIn and In^-) can satisfactorily monitor the pH inside the monoliths [8–11]. In general HIn's present distinct bands for the acid and base pairs, in Supplementary material Table 1, properties of the dyes used in this work are revised for the sake of clarity.

The prototropic equilibria of the pH dyes (HIn's) were monitored during 55 days after the preparation of the monoliths. In Supplementary material Fig. 1(A–E), dyes typical UV–vis absorption spectra as a function of the buffer concentration after the first day of monolith preparation is presented. The data shows that the contribution of the forms HIn and In^- are in accordance with the nominal starting pH presented in Table 1. Spectra of the dyes did not change with the aging and also with the shrinkage showing a "constancy" of pH at least from the viewpoint of the dyes equilibria. Only small variations in the absorption wavelength

Table 1
Calculated pH's inside the TEOS monoliths.

[Buffer] in monoliths (mM)	$pH_{calc.}$
50	5.81
40	5.75
30	5.63
20	5.17
5	3.15

maxima of the dyes with the aging can be noticed. Red shifts on the absorption maxima of the acid species (HIn) are noticed, whereas for the basic species (In^-) blue shifts are observed. These effects are in accord with the increase in polarity inside the gel as previously found [8,10–12].

The gel preparation (see material and methods) initiated with the pre-hydrolysis of TEOS (in the presence of 2 mM HCl) followed by the addition of appropriate amounts of phosphate buffers (see figure captions). It should be added that this protocol was chosen to follow previous works [6] and therefore the initial pH was expected to vary with the amount of added buffer, that is its buffer capacity. Straightforward calculations of the starting pH conditions (concentration of HCl and of phosphate buffer inside the monoliths) are shown in Table 1. These values are in agreement with the dyes spectra presented in Supplementary material Fig. 1. It should be added that the effect of increased ionic strength due to the gel shrinkage on the re-association equilibrium of In^- is also observed leading to a decrease of the dyes pKa's in agreement with the previous work [13] (data not shown).

4.2. Pyranine ESPT in bulk and in gels

Typical absorption and emission spectra of pyranine in acidic, basic and in pure water are presented in Fig. 1A and B. As included in Scheme 1, absorption and emission maxima are clearly seen. In acid media, absorption of POH is centered at 403 nm whereas in basic media absorption is centered at 455 nm. Emission spectra clearly show the bands at 445 nm (POH) and at 510 nm (PO^-) and also the contribution of either one of the species as shoulders to the main band as a function of the pH (see Scheme 1).

Pyranine photodissociation is highly sensitive to the water content in a mixture and is therefore an appropriate probe to monitor sol–gel processes, as illustrated in Fig. 2A and B for a 7 days aged gel. Fig. 2A depicts the absorption spectra of pyranine using the various concentrations of the phosphate buffer (see Fig. 2 caption and Table 1). The main contribution of POH ground state species (λ=403 nm; Fig. 2, inset) as well as the small ones due to the PO^- (λ=450 nm; Fig. 2, expanded spectra) is observed. It can be noticed that as the pH increases the extent of PO^- augments in accordance with the pyranine pKa and the pH of the gel (Table 1). Absorption spectra were monitored during 77 days and showed no other changes except for small blue and red maxima shifts for POH and PO^- bands respectively (as observed for the pH dyes) showing an increase in the medium polarity. This effect is attributed to the increase in the ionic strength due to the gel shrinkage and to a larger polarity around the probes due to gel network formation as well.

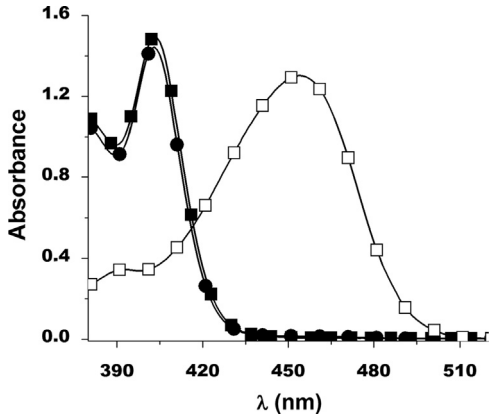

Fig. 1. Absorption (A) and emission (B) spectra of pyranine in (■) acidic, (▲) basic and (○) aqueous media.

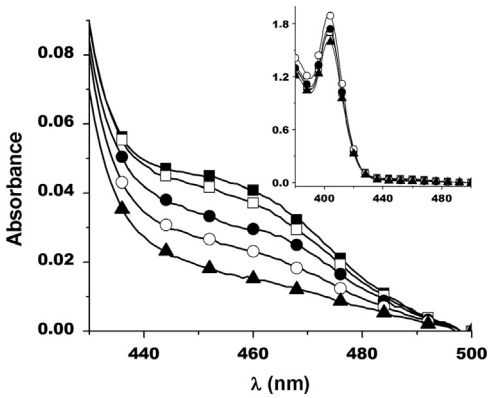

Fig. 2. Expanded absorption spectra of pyranine at the 440–480 nm region as a function of buffer concentration and pH in 7 days aged TEOS monoliths in (■) 50 mM; (○) 40 mM; (▲) 30 mM; (□) 20 mM and (□) 5 mM phosphate buffer. Inset: absorption spectra of pyranine in 7 days aged gels as function of buffer concentration and pH.

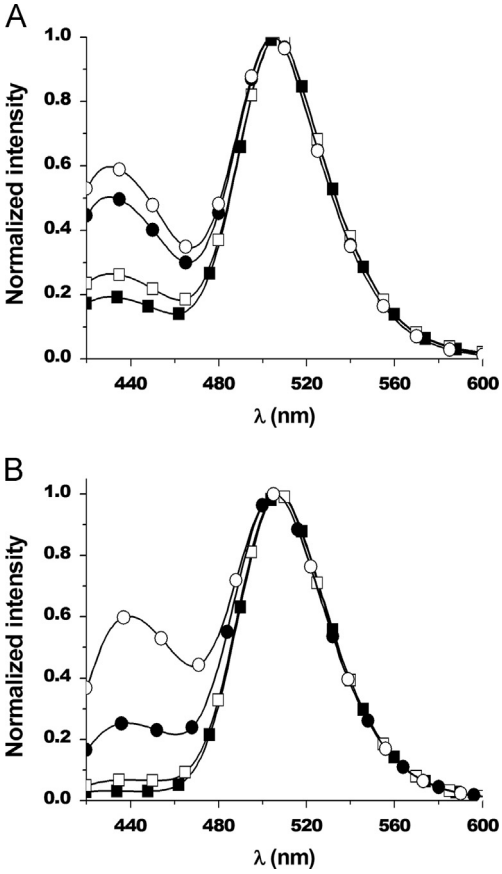

Fig. 3. Normalized fluorescence emission spectra of pyranine included in TEOS derived monoliths in (●) 250, (■) 50, (□) 5, and (▲) 0.5 mM pH=6.0 phosphate buffer after 1 (A) and 51 (B) days of preparation.

Representative normalized fluorescence emissions of TEOS monoliths as a function of aging and buffer concentration are depicted in Fig. 3A and B. It can be observed in these assays conditions (see Fig. 3 caption) that: (i) In Fig. 3A, the increase in the POH contribution (λ=445 nm) as the buffer concentration decreases. Notice that as the spectra are normalized the intensity at λ=510 nm (PO^-* contribution) remains fixed whereas that due to POH augments. In other words the extent of ESPT (see Scheme 1) diminishes and (ii) in Fig. 3B the equivalent contributions of POH but for a 51 days aged gels. Comparing the two

figures it is clear that there is an increase in ESPT (decrease in the relative POH contribution) for the same initial conditions with aging.

Analysis of the relative fluorescence intensities, as those presented in Fig. 3, can result in a more comprehensive understanding by plotting the percentage of PO^{-}* (% PO^{-}*). Where % PO^{-}* is the relative amount of photo-dissociated pyranine for the gel samples with the buffer concentrations studied (Table 1) as a function of the aging process. The amount of PO^{-}* is calculated from the emission spectra, taking the ratio of the emission intensity due to PO^{-}* and the sum of the intensities due to PO^{-}* ($I_{(PO^{-}*)}$) and POH* ($I_{(POH^*)}$). Several studies have presented ways to best correct the emission profiles in order to properly calculate the extension of photodissociation [14], however for the present work the equations below are sufficient. This treatment arises from the analysis of the relative emission intensities and allows canceling effects from the gel shrinkage and the experimental difficulties in positioning the samples in exactly the same position in the instrument. The % PO^{-}* is determined by the equation (notice that POH is the main species in the ground state and the emission at 510 nm due to PO^{-}* arises from the ESPT),

$$\%\ PO^{-}* = I_{(PO^{-}*)}/[I_{(PO^{-}*)} + I_{(POH^*)}]$$

Quantum yields of POH and PO^{-} in the gels are found equivalent to that in the solution by direct comparisons of the absorption and emission spectra of them. In other words control aqueous solutions (either 6 M $HClO_4$ or NaOH 1 mM) presented the same absorption and emission spectra as those gels having either one of the species. Considering therefore the known condition that the sum of the quantum yields for pyranine species is close to one [5]

$$(\Phi_{POH} + \Phi_{PO^-})/(\Phi_{POH^0} + \Phi_{PO^{-0}}) = 1$$

where Φ_{POH}, Φ_{PO^-}, $\Phi_{POH}{}^0$ and $\Phi_{PO}{}^{-0}$ are the fluorescence quantum yields of POH and of PO^{-}* in the presence and absence of excited state reactions, respectively [5]. Once again by taking into account that in the experimental pH's, the main species in the ground state are POH (Fig. 2), the following approximation is valid:

$$(\Phi_{POH}/\Phi_{PO^-}) \sim (I_{510}/I_{445}) = R$$

the extension of dissociation (% D) can be defined as

$$\%\ D = (I_{510}/I^0_{445})$$

and therefore

$$\%\ PO^{-}* = (R/(1+R))$$

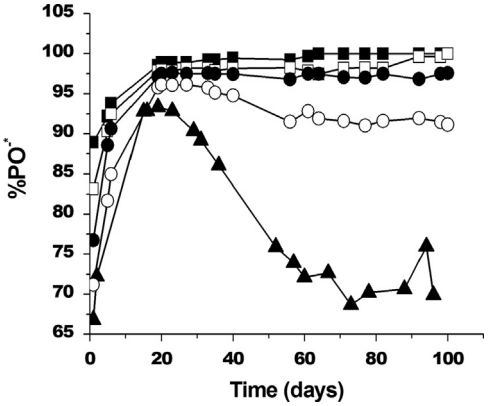

Fig. 4. Percentage of pyranine dissociation (% PO^{-}*) as function of aging in TEOS derived monoliths in (•) 250, (■) 50, (□) 5, and (□) 0.5 mM, pH=6.0 phosphate buffer and in pure H_2O ( ). Data were calculate in accord to the % $PO^{-}{}^{*}$ equation (see text) for data as in the figure.

4.3. Extent of ESPT in aged gels

In Fig. 4 it is observed that the % PO^{-}* increases up to the 22nd aging day for the buffer concentrations studied, leveling off for phosphate concentrations equaling 0.05 and 0.04 M and decreases for the others. An initial increase in % PO^{-}* is observed within the time of the sol–gel preparation till about 1 day aging (data not shown). This effect derives from the ethanol exudation process from the gel matrix (notice that ethanol prevents ESPT). The initial gel condition contains a mixture of H_2O and ethanol (TEOS hydrolysis products) within the sol–gel matrix, simple tests revealed that ethanol is the first to lixiviate through the gel and appears in the compartment between the cell walls and the gel itself that is beginning to contract (water loss during the aging is presented below) [15]. In consequence, as the ethanol fraction decreases the ESPT increases, thus augmenting the PO^{-}* emission intensity.

These observations are in contradiction to the previous report by Brennan, who claimed a re-hydration process of the gel by long standing [6]. Present findings show instead the participation of the buffer species in the prototropic process above a threshold concentration. Accordingly, in the present study it is found that above 0.05 M, buffer acidic species participate in the process keeping the amount of PO^{-}* constant even after 77 days aging. Before continuing the analysis it is necessary to tackle the question on the decrease in the gel water content, which was aged in vials open to the air. The decrease in the water mole fraction will lead to increased ionic strength concentration of the buffer species and, therefore, in their associated effects on the prototropic process.

4.4. Ionic strength effect on laser pH-jump pyranine reprotonation

First let us address the ionic strength effect due to the gel shrinkage by monitoring the ground state reprotonation process via a laser induced pH jump [3]. In these experiments the re-association (protonation) kinetics of PO^{-}, formed after the ESPT and the PO^{-}* decay, is measured (see Scheme 1). In Supplementary material Fig. 2 typical o'scope traces of 2 and 19 days aged gels are shown. For a 2 days aged gel between 0.22 and 0.3 μs , the scattering of the laser pulse plus fluorescence emission and PMT recovery are observed, and true re-association signals start around after 0.32 μs. Signals for a 19 days aged gels show faster kinetics (Fig. 2 Supplementary material). Independent of the low signal to noise ratios in these data it is clear that the aging of the gel leads to faster reprotonation kinetics. This “acceleration” is attributed to the gel shrinkage that approximate the reaction partners, it should be added however that the increase in the ionic strength (μ) due to the shrinkage goes in the opposite direction once the Debye radii decreases with μ. In other words increase in μ leads to smaller rate constant values. In Table 2 selected data for the reprotonation rate constants in water, in 2 and 5 days aged gels are presented. Data in pure water (Table 2, column 2) show the increase in the observed rate constants as a function of the increase in the buffer concentration. The overall effect is, therefore, due to the increase in H-

Table 2
Pyranine Reprotonation (k_{ass}) rate constants in, H_2O, and in 2 and 5 days aged gels.

[Buffer] (mM)	H_2O	$k_{ass} \times 10^6\ M^{-1}\ s^{-1}$	
		2 days	5 days
50	2.80	4.48	6.42
40	2.12	4.01	5.50
30	1.56	5.18	9.72
20	0.89	10.70	28.90
5	0.25	72.23	173.00

donating species concentration (acid form of the phosphate buffer) which leads to a rate constant enhancement, diminished by the effect of increase in the ionic strength which leads to a decrease in the reaction rate constant. Taking into account μ's, buffer concentrations, and pH's in the gel, calculation of these effects on the observed rate constant can be fully realized using known models (14). For the scope of this study, however, it is more important to focus only on the shrinking effect of the gel on the reprotonation rate constant, that is by considering data in the same row in Table 2. Clearly, rates increase with the gel shrinkage caused by the approximation of the H-donating species towards PO^-.

4.5. Water loss from gel shrinkage

An important issue concerning pyranine reprotonation kinetics is to get information on the amount of water present inside the gel. This information can be obtained by measuring the loss of solvents during the aging process. As presented above, in the assay conditions, ethanol initially lixiviates from the gel and only after 1 day water begins to be exuded during the shrinkage process [15]. Accordingly after removal of the ethanol (with the aid of syringe), the measurement of the mixture weight following 1 day of aging is thus a reasonable measurement of the water loss.

In Fig. 5 the percentage loss of weight is presented for the gels having the four phosphate buffer concentrations studied. It can be seen that the gels behave in a parallel fashion and up to 135 days the weight loss is about 80%. These data reinforce the explanations of the effect of the phosphate buffer species acting as H-donor to PO^- reprotonation kinetics (Table 2) as well the steady state fluorescence data (Figs. 3 and 4)

4.6. Pyranine ESPT process in solid matrices (phosphate and sodium chloride)

In order to further exploit the H^+-transfer in solid matrices, pyranine fluorescence was monitored in solid and dry mixtures of phosphate buffer components and also in pure NaCl (see materials and methods). In crushed mixtures with KH_2PO_4/K_2HPO_4 proportions for apparent pH's of 6.0, 5.8, 5.4, 5.0, 4.7, 4.3 and 4.0 (appropriate amounts of each buffer component were weighed to the nominal pH and total concentration of 0.05 M as in aqueous solutions) and the normalized emission spectra data are presented in Fig. 6. It can be observed that the emission at the POH region ($\lambda \sim 440$ nm) increases with the decrease in the apparent pH. This result could derive from either a decrease in ESPT or a decrease in the ground state equilibrium pKa.

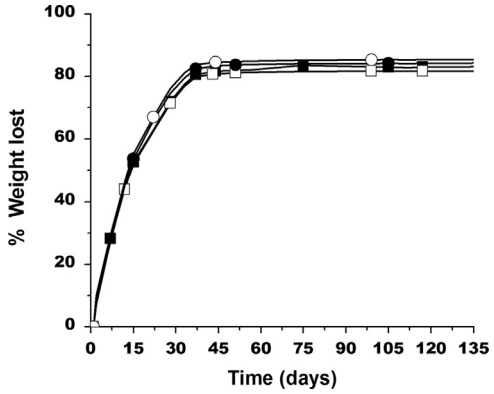

Fig. 5. Water percentage weight lost from the TEOS monoliths as function of the time for the concentration (•) 250 mM; (■) 50 mM; (□) 5 mM; (□) 0.50 mM phosphate buffer.

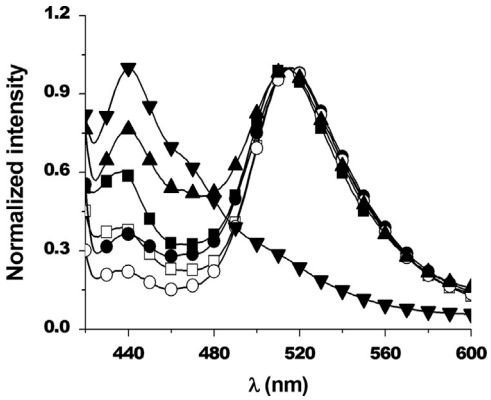

Fig. 6. Normalized fluorescence emission spectra ($\lambda_{exc.}=380$ nm) of pyranine in dry mixtures of KH_2PO_4 and K_2HPO_4 as function of the $pH_{apparent}$ (■) 6.0; (○) 5.8; (▲) 5.4; (□) 5.0; (□) 4.7; (●) 4.3 e (□) 4.0.

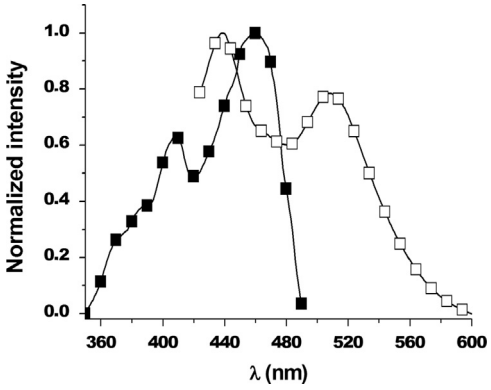

Fig. 7. Fluorescence excitation spectra ($\lambda_{em.}=540$ nm) (■) and fluorescence emission spectra (○) ($\lambda_{exc.}=380$ nm) of pyranine in dry NaCl.

To tackle this question the fluorescence emission and excitation spectra of pyranine in solid NaCl, a non protic medium with lack of H^+ acceptors or donors species, were recorded (Fig. 7). With the emission monochromator set at 540 nm, excitation peaks appear at ~410 nm and ~450 nm (Fig. 7, left trace) and with the excitation set at 380 nm, emission bands appear at $\lambda_{exc}\sim 440$ nm and ~520 nm, respectively (Fig. 7, right trace). These spectra show the presence of both POH and PO^- in the ground state where maxima's red shifts compared to the values in water are due to the higher medium polarity. Thus in solid and dry NaCl where ESPT cannot occur, pyranine acid base pair co-exists.

For the experiments in phosphate solid (Fig. 6) the same co-existence of POH/PO^- species prevails. Thus as the "nominal" pH decreases, the amount of POH augments and an apparent pKa about 4.7 can be inferred (Fig. 6, inset). Accordingly in dry KH_2PO_4/K_2HPO_4 no ESPT process occurs and the spectral behavior is a direct representation of the initial ground state probe species concentrations.

The effect of the increase in the amount of water to allow the establishment of a quasi equilibrium condition for ESPT reaction in $HPO_4^=/H_2PO_4^-$ with a nominal pH of 6.0 is presented in Fig. 8. In the first condition (no water), the excitation spectrum shows only a residual emission at 540 nm but from the 450 nm region. Increase in water concentration is accompanied by an increase in the excitation at the POH absorption band region. It is found that the extent of pyranine prototropic equilibrium seen by the increase in POH excitation band and emission set at 540 nm grows as a function of the water content, and levels off at around 0.75. This is the same threshold observed in the drying aging of TEOS (Fig. 4) where % PO^-* remains constant by the participation of the buffer salt species in the ESPT reactions thereafter (Fig. 4).

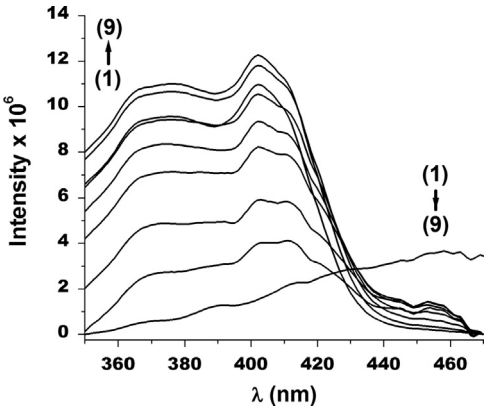

Fig. 8. Normalized fluorescence excitation spectra ($\lambda_{em.}$=540 nm) of pyranine in dry mixtures of KH_2PO_4 and K_2HPO_4 $pH_{aparent}$=6.0 as function mole fraction water $X_w \times 10^{-3}$ (■) 0.22; (○) 0.36; (▲) 0.46; (□) 0.53; (□) 0.59; (●) 0.63; (□) 0.69; (▼) 0.74 and (◂) 0.76.

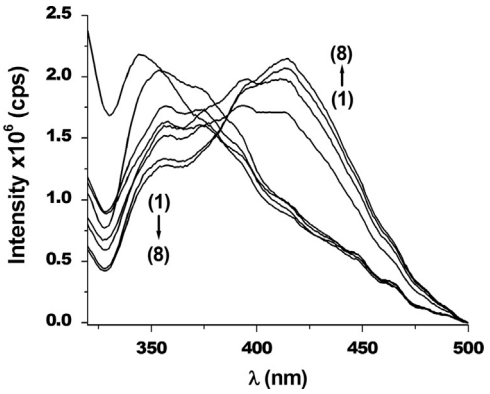

Fig. 10. Normalized fluorescence emission spectra ($\lambda_{exc.}$=294 nm) of 2-naphthol in dry mixtures of KH_2PO_4 and K_2HPO_4 with $pH_{aparent}$=6.0 as function of water mole fraction ($X_w \times 10^{-3}$) (1) without; (2) 0.19; (3) 0.31; (4) 0.44; (5) 0.53; (6) 0.56; (7) 0.61; (8) 0.63.

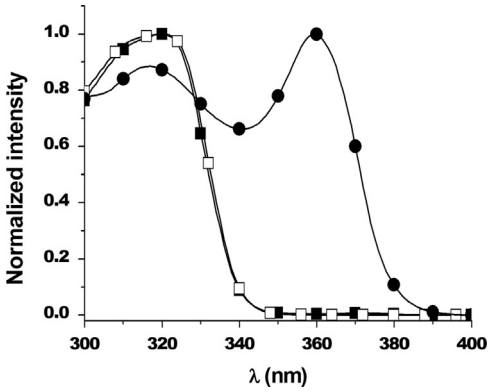

Fig. 9. Normalized fluorescence excitation spectra ($\lambda_{em.}$=430 nm) of 2-naphthol in (■) acidic (pH 1), (▲) basic (pH 10) and (○) aqueous media.

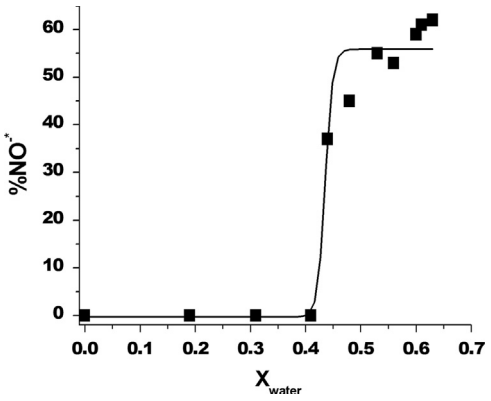

Fig. 11. Prototropic dissociation degree (% NO^{-}*) of 2-naphthol as function of mole fraction water in dry mixtures of KH_2PO_4 and K_2HPO_4.

4.7. ESPT of 2-naphthol in phosphate matrices

Another photoacid, 2-naphthol (2-NOH) was studied for data comparisons. 2-NOH has a ground state pKa=9.5 and an excited state pKa=2.8 [1,2]. These pKa's values are appropriate to investigate the ESPT reactions in $HPO_4^{=}/H_2PO_4^{-}$ mixtures at pH values where the acid form of 2-naphthol is the dominant species in the ground state and the ESPT reactions, if allowed, will dominate. Typical excitation and emission spectra of 2-NOH are presented in Fig. 9. The acid and basic species present excitations maxima at 320 nm and 360 nm, respectively; and emissions at 355 nm and 420 nm, respectively. By excitation at an appropriate wavelength, and monitoring the emission spectra, similar to pyranine, the extent of ESPT can be monitored. Similarly, with pyranine, emission intensities of both 2-NOH and 2-NO^{-}* in the gels are close to that in the aqueous solution, and, therefore, the percentage of NO^{-}* (% NO^{-}*) can be estimated as well. In Fig. 10 the effect of water addition in solid and dry phosphate is presented. The observed increase in the emission due to basic form ($\lambda \sim 420$ nm) confirms the growth of the ESPT process. The calculated % NO^{-}* as a function of the water mole fraction (X_w) is plotted in Fig. 11. As found with pyranine a minimum amount of 0.4% water mole fraction (X_w) is necessary for the prototropic equilibrium to occur (ESPT reaction), and it further levels off above 0.5% X_w (see Scheme 2).

Excitation of ROH leads ROH towards the conjugated base (**1**) for the formation of the geminate ion pair RO^{-}*H^{+}. With suitable H_2O molecules (**χH_2O**), the geminate ion pair (|**RO^{-}***H^{+}|) goes to the respective solvent separated ion pair (|**RO^{-}***|||H^{+}|) (**2**). Decay of

ROH

↓ hν

ROH* = [---||RO-*H+||--] + χH2O = [--|RO-*||||H+|--] = [(R-O-*)aq]

(1) (geminate ion pair) (2) (solvent separated ion pair)

↓ excited state acid decay ↓ excited state base decay

[(R-O-)aq] + [(H+)aq]

(3) coupled proton reactions ↓↑ ↓↑

(H2PO4-)aq (HPO4=)aq

χ ≥ 0.4 %

(χ - Water Molar Fraction in Solid Matrices)

Scheme 2. Summary model equations for ESPT process in Vitreous and Solid Phases.

the free base RO^{-}* generate the free ions (**[(R–O^{-})aq]+[(H^{+})aq]**) that can undergo proton transfer reactions with the buffer species (**($H_2PO_4^{-}$)aq** and **($HPO_4^{=}$)aq**) (**3**). Minimum water is above **$\chi \geq 0.4\%$** for photodissociation.

5. Concluding remarks

In the present study the effect of water loss due to aging of TEOS monoliths exposed to air is focused. Data is obtained by

monitoring photoacids H^+-transfer processes. It is shown that the contraction of the gel increases the concentration of buffer components in the ESPT process both as an acceptor as well as a H^+ donor species. This effect leads to a constancy in the extent of photodissociation seen by the amount of the emission of excited state basic species. However when the amount of water in the gel is in a limit of ~20% the photoacid behavior is interrupted. Parallel studies with solid mixtures constituted by either buffer species or sodium chloride reveal the same properties that are an increased effect of acid and basic components in the H^+-transfer but with the same minimum amount ~0.4% X_w of the carrier H_2O molecules. In conclusion excited state H^+ transfer depends on the presence of water to generate the geminated solvated ion pair [–||RO^-*H^+||–], the separated solvated ion pair [–RO^-*|||H^+–], and finally the free ions [RO^-*] and [H^+]. The presence of other H^+ proton donor and acceptors species can participate in the kinetics and to a leveling off effect and in the recombination ground state kinetics as well (Scheme 2).

Acknowledgments

We wish to express our deep gratitude to the Brazilian granting agencies CAPES, CNPQ and FAPESP. This work was part of the FACS master dissertation.

Appendix A. Supporting information

Supplementary data associated with this article can be found in the online version at http://dx.doi.org/10.1016/j.jlumin.2013.09.038.

References

[1] T. Förster, Naturwissenschaften 36 (1949) 186;
T. Förster, Zeitschrift fuer Elektrochemie 54 (1950) 42;
A. Weller, Progress in Reaction Kinetics 1 (1961) 189.
[2] V. Kaufmann, D. Huppert, M. Gutman, Chemical Physics Letters 64 (1979) 522;
D. Huppert, E. Kolodney, Chemical Physics 63 (1981) 401.
[3] J. Mckiernan, E. Simoni, B. Dunn, Z.I. Zink, Journal of Physical Chemistry 98 (1994) 1006.
[4] V. Kaufman, D. Avnir, D. Pines- Rojanski, D. Huppert, Journal of Non-Crystalline Solids 99 (1988) 379.
[5] C. Fernandez, M.J. Politi, Journal of Photochemistry and Photobiology A 104 (1997) 165;
C. Fernandez, Journal of the American Chemical Society 104 (1984) 5352;
P. Leiderman, A. Uritski, D. Huppert, Journal of Physical Chemistry A 111 (2007) 4998.
[6] K.K. Flora, M.A. Dabrowski, S.P. Musson, J.D. Brennan, Canadian Journal of Chemistry 77 (1999) 1617.
[7] N.K. Chaudhury, R. Bhardwaj, B.M. Murari, Current Applied Physics 3 (2003) 177.
[8] Avnir, Kaufman, Journal of Non-Crystalline Solids 192 (1987) 180.
[9] C. Rottman, M. Ottolenghi, R. Zusman, O. Lev, M. Smith, G. Gong, M.L. Kagan, D. Avnir, Materials Letters 13 (1992) 293.
[10] Rivka Zusman, Claudio Rottman, Michael Ottolenghi, David Avnir, Journal of Non-Crystalline Solids 122 (1990) 107.
[11] Claudio Rottman, Avner Turniansky, David Avnir, Journal of Sol-Gel Science and Technology 13 (1998) 17.
[12] Enju wang, Kwok-Fan Chow, Vivian Kwan, Tammy Chin, Crystal Wong, Andrew Bocarsly, Analytica Chimica Acta 495 (2003) 45.
[13] R.P. Hideo Yamazaki, Sperline, Henry Freiser, Analytical Chemistry 64 (1992) 2720.
[14] Y. Avnir, Y. Barenholz, Analytical Biochemistry 347 (2005) 34.
[15] M.J. Politi, C.D. Tran, Journal of Non-Crystalline Solids 304 (2002) 64.